

This article was downloaded by:

On: 25 January 2011

Access details: *Access Details: Free Access*

Publisher *Taylor & Francis*

Informa Ltd Registered in England and Wales Registered Number: 1072954 Registered office: Mortimer House, 37-41 Mortimer Street, London W1T 3JH, UK



Separation Science and Technology

Publication details, including instructions for authors and subscription information:

<http://www.informaworld.com/smpp/title~content=t713708471>

Performance Analysis of a Continuous Rotating Annular Electrophoresis Column

R. A. Yoshisato^a; L. M. Korndorf^{a,b}; G. R. Carmichael^a; R. Datta^a

^a Department of Chemical and Materials Engineering, The University of Iowa, Iowa City, Iowa ^b John Deere Technical Center, Moline, Illinois

To cite this Article Yoshisato, R. A. , Korndorf, L. M. , Carmichael, G. R. and Datta, R.(1986) 'Performance Analysis of a Continuous Rotating Annular Electrophoresis Column', *Separation Science and Technology*, 21: 8, 727 – 753

To link to this Article: DOI: 10.1080/01496398608056147

URL: <http://dx.doi.org/10.1080/01496398608056147>

PLEASE SCROLL DOWN FOR ARTICLE

Full terms and conditions of use: <http://www.informaworld.com/terms-and-conditions-of-access.pdf>

This article may be used for research, teaching and private study purposes. Any substantial or systematic reproduction, re-distribution, re-selling, loan or sub-licensing, systematic supply or distribution in any form to anyone is expressly forbidden.

The publisher does not give any warranty express or implied or make any representation that the contents will be complete or accurate or up to date. The accuracy of any instructions, formulae and drug doses should be independently verified with primary sources. The publisher shall not be liable for any loss, actions, claims, proceedings, demand or costs or damages whatsoever or howsoever caused arising directly or indirectly in connection with or arising out of the use of this material.

Performance Analysis of a Continuous Rotating Annular Electrophoresis Column

R. A. YOSHISATO,* L. M. KORNDORF,† G. R. CARMICHAEL, and R. DATTA

DEPARTMENT OF CHEMICAL AND MATERIALS ENGINEERING
THE UNIVERSITY OF IOWA
IOWA CITY, IOWA 52242

Abstract

A new continuous electrophoresis column is proposed which will allow for the continuous separation of industrial scale multicomponent mixtures. Computer simulated calculations predict steady-state bed temperature, separation distance, and power requirements. The proposed design compares favorably to previous designs in terms of minimizing peak bed temperature and power consumed.

INTRODUCTION

Recent advances in genetic engineering and related biotechnology have allowed the development of chemical products never before commercially feasible. In other cases, this new technology has been exploited to improve the purity, activity, or profitability of already existing products. Several years ago, Eli Lilly began marketing a biosynthetic human insulin synthesized using recombinant DNA technology, and Genentech has developed a commercial method for producing human growth hormone. Other products on the horizon include β -interferon and interleukin-2. However, the industrial use of these biotechnological developments is yet in its infancy. If these biotechnology advances lead to the large-scale synthesis of commercial

*To whom correspondence should be addressed.

†Present address: John Deere Technical Center, Moline, Illinois 61625.

products, current separation and purification techniques will need to be adapted and refined to process these products.

Electrophoresis is a powerful and extremely versatile method for the separation of biochemicals. It exploits the different electrophoretic migration velocities of charged species under the influence of an electric field. Electrophoresis was originally used in the separation of proteins (1). Since then it has been used to separate a variety of products including ions, dyes, colloids, cellular material, organelles, and whole cells (2-5). In fact, there is hardly a class of compounds which has not been separated by electrophoresis. Thus, electrophoresis is a good candidate for the downstream separation and purification of products from bioprocesses. Advantages include the good resolution possible for the separation of bioproducts and the ability to maintain the bioactivity of these products.

There are several methods for implementing an electrophoretic separation including moving boundary, zone, isotachophoresis, and isoelectric focusing. Each of these methods is well described in a number of texts (6-11). Dobry and Finn (12) reviewed the use of electrophoresis up to the late 1950s and proposed the development of a large-scale continuous electrophoretic device for industrial applications. Some of the problems which limited the use of electrophoresis for large-scale separations included: batch operation limited system throughput and capacity, excessive temperature rise by Joule heating which could damage products, and hydrodynamic effects including turbulence and natural convection which could remix separated products. Other phenomena now known to limit separation power potentially are electroosmosis, thermal and simple diffusion, nonuniform flow profile, Kohlrausch-type phenomena, Taylor-type dispersion, and electroturbulence (5, 13-18).

In order to achieve increased throughput, continuous free-flow zone electrophoresis systems were developed by Philpot (1) and by Hannig (19, 20) and Strickler (21). Both methods have eluent flowing in the narrow gap between flat parallel plates. The gap is typically between 0.5 and 1.0 mm, ensuring laminar flow of eluent. In the case of the Philpot method, a voltage gradient is applied across the gap, perpendicular to the eluent flow, whereas the Hannig method uses a voltage gradient applied along the length of the gap, still perpendicular to the eluent flow. In the Philpot method, fractions of different electrophoretic mobility are collected across the narrow width of the gap, while the Hannig method requires fraction collection along the length of the gap. Without a specially designed collection mechanism, the separation of a sample into many fractions in a Philpot device is limited by the narrowness of the gap. As a result, until recently, much of the work in continuous free-flow electrophoresis has been based on the Hannig design (2, 4, 21).

Despite continuous operation of the Hannig electrophoresis method, the throughput is still rather modest, typically less than 10 mL/h for protein separations (16, 22). Larger throughputs are possible in large gap devices. Generally, these devices have been considered unsuitable due to excessive temperature rise from Joule heating. Work with large gap annular columns was initiated by Vermeulen and coworkers at Berkeley (23), and a 37.7-L continuous electrophoresis column was later developed (24). The device had an annular gap of approximately 8.4 cm and was capable of processing up to 1000 g/h of a binary feed stream. Due to the position of the electrodes at the centerline and along the circumference, the separation occurred in the radial direction with fractions being collected along the radial coordinate. As a result, multicomponent or difficult to separate components require a thick bed in order to achieve good resolution. However, larger bed thicknesses increase the amount of Joule heating and decrease the heat transfer efficiency. Thus, the bed is limited to 5 to 10 cm in order to prevent thermal degradation of the product.

Although the throughput can be increased to industrial levels in thick-bed electrophoresis devices, band-broadening effects can be more profound, leading to lower resolution and inadequate separating power. Hannig and coworkers (16) have surveyed such phenomena in free-flow electrophoresis. Depending on the geometry of the device and the orientation of the electric field to the bulk velocity, the interaction of the electroosmotic flow and the laminar velocity profile can lead to the separated bands taking on a curved cross section known as the crescent phenomenon (21). This effect can be attenuated and the bands sharpened by adjusting the wall zeta potential (13, 14).

More important in thick-bed devices is the increased Joule heating and reduction in heat transfer efficiency which can lead to the formation of substantial temperature gradients in the bed. These temperature gradients can cause natural convection currents and other hydrodynamic instabilities which can distort the separated bands. Dobry and Finn (25), in their early experimental work, attempted to suppress eddies due to buoyancy effects through forced convection and the use of thickening agents such as dextran which increased fluid viscosity by a small amount. The premise was that the relative effects of natural convection would then be reduced without appreciable affect on the rest of the process. A theoretical study of the interaction of the various types of convection in a rectangular electrophoresis channel was initiated by Ostrach (26). He developed a number of correlations involving Reynolds number, Grashof number, and Rayleigh number. Since then more detailed hydrodynamic models have been developed to simulate the temperature and flow fields in Hannig-type electrophoresis columns (27, 28).

Despite the body of work on Hannig-type devices, a continuous preparative electrophoresis device has recently been developed based on the Philpot method at Harwell under the auspices of the United Kingdom Atomic Energy Authority (29). The Philpot/Harwell unit is capable of separating up to 30 fractions at flow rates of 20 mL/min. It operates adiabatically with a temperature rise of 20–25°C between inlet and outlet streams; however, contact time is 30–60 s and thermal degradation is therefore minimized. Flow occurs through a thin 5 mm annulus. Convection instabilities are minimized by rapidly rotating the outer wall relative to the stationary stator at the center to maintain an angular laminar velocity profile. Separation occurs in the radial direction with sample entering through the base of the stator and product being carefully removed at the top through a set of 30 circular disks of various radii.

CONTINUOUS ROTATING ANNULAR ELECTROPHORESIS COLUMN

The continuous rotating annular electrophoresis (CRAE) column shown in Fig. 1 is a new approach to large-scale electrophoresis, different from the Hannig-type devices as well as the Philpot/Harwell unit. In the CRAE column an electric field is imposed axially in a thick-bed annular column, along the same direction as eluent flow, while the annular bed is rotated slowly about its axis. Sample and eluent introduction ports at the top of the column are fixed in space as well as the multiple product collection ports which ring the circumference at the bottom of the column. As a result of this configuration, separated fractions appear as helical bands as shown in Fig. 2. Each component leaves the column at a different angular position. Since the separation takes place in the angular direction rather than the radial direction as in Vermeulen's column, the bed may be kept relatively thin to improve heat transfer and reduce the peak bed temperature rise. This should also reduce the temperature gradient and thereby reduce the flow instabilities due to buoyancy effects. The column may also be packed or the viscosity increased to further reduce natural convection. A rotating device of similar geometry has already been successfully used in the chromatographic separation of multicomponent mixtures (30–36). A general theory for continuous rotating annular separation processes has been studied by Wankat (37, 38).

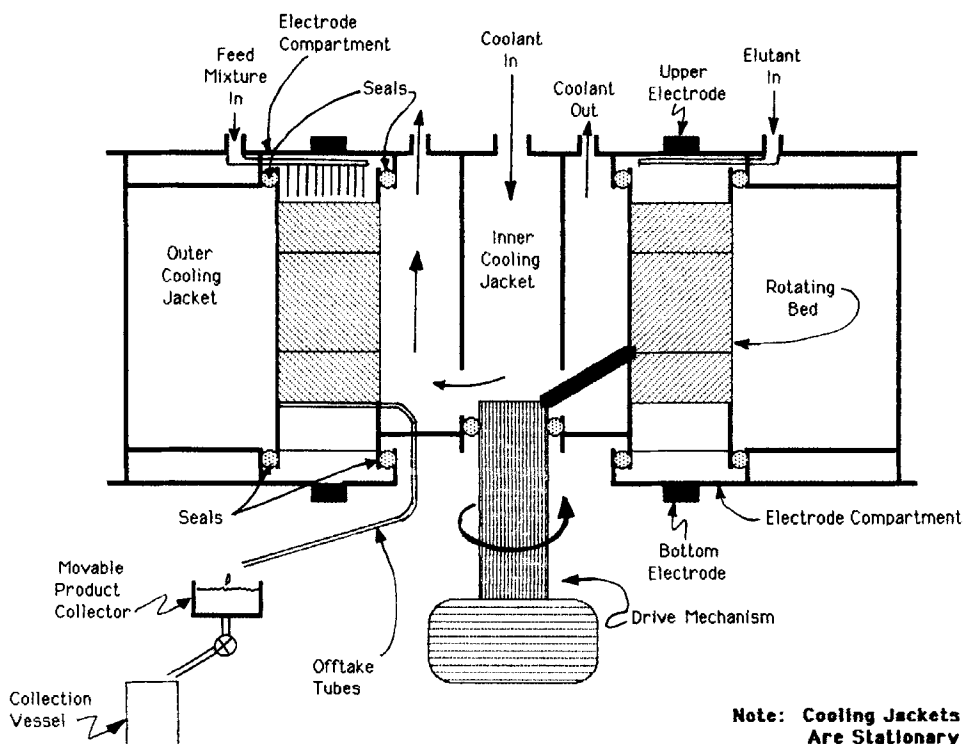


FIG. 1. Schematic of the continuous rotating annular bed column for electrophoresis.

For relatively thick-bed devices like the CRAE column, large temperature gradients and related buoyancy effects are a significant reason for loss of resolution. Considerable work has been done on estimating the temperature profile and heat transfer in electrophoresis columns (39-43). The present study is concerned with the simulation of the temperature profiles, the separation distance, and the power requirements for the CRAE column. The results of the simulation are then compared with the Vermeulen column to serve as an initial measure of the feasibility of the CRAE column as an electrophoretic separator. The Vermeulen column is used for comparison purposes since it is also a thick-bed annular design capable of preparative scale separation. Rectangular Hannig-type devices are thin-bed designs which still suffer from low throughput and would not be directly comparable. Due to its novel design, the Philpot/Harwell unit is not used for initial comparisons.

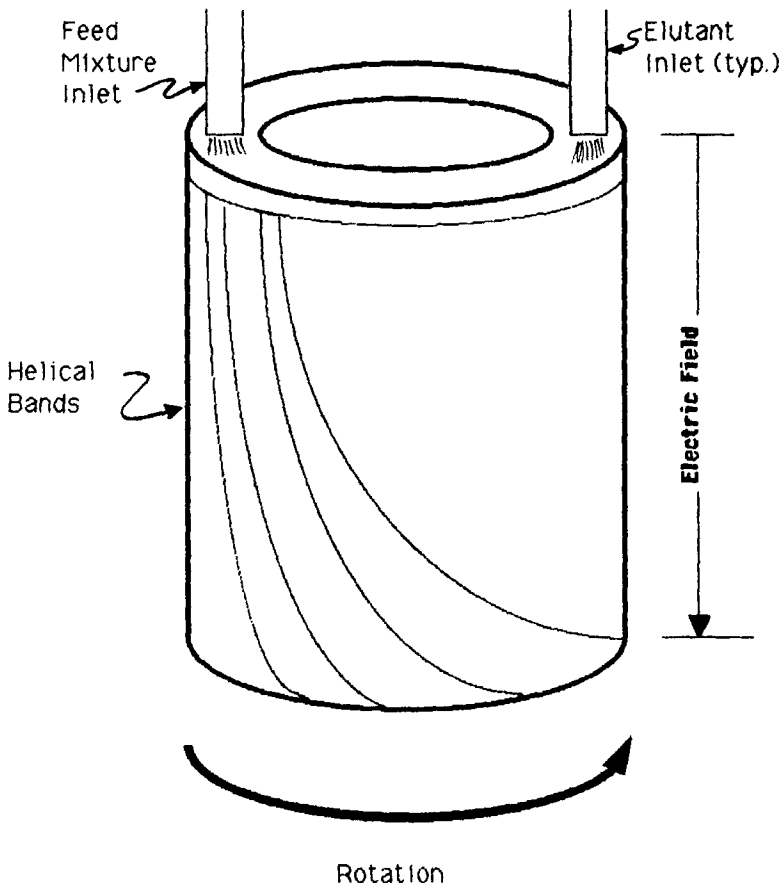


FIG. 2. Helical bands in a CRAE column.

The preliminary model is limited to plug flow in an annulus with constant temperature boundary conditions. Band spreading by simple diffusion is considered; however, dispersion effects as a result of feed flow rate and inlet port design are not considered. Hydrodynamic interactions as a result of natural convection, turbulence, and electroosmosis are considered in a more detailed model to be experimentally verified and published later.

THEORY

Temperature Profile

The temperature profile developed in the CRAE column is obtained through application of the thermal energy balance (44).

$$\frac{\partial(\rho C_p T)}{\partial t} = \nabla \cdot k_h \nabla T - \nabla \cdot (\rho C_p T \langle v \rangle) + \mathbf{i} \cdot \nabla E \quad (1)$$

With the following assumptions:

Steady state

Convection only in the axial direction

Axial conduction negligible relative to axial convection

Constant axial velocity $\langle v \rangle$

Constant physical properties in the bed, ρ, C_p, k_h, k_m

Constant wall temperature

Equation (1) becomes

$$\frac{k_h}{r} \frac{\partial}{\partial r} \left(r \frac{\partial T}{\partial r} \right) - \langle v \rangle \rho C \frac{\partial T}{\partial z} + \mathbf{i} \cdot \nabla E = 0 \quad (2)$$

with boundary conditions

$$T = T_0 \text{ at } z = 0 \quad (3)$$

$$T = T_0 \text{ at } r = r_a \quad (4)$$

$$T = T_0 \text{ at } r = r_b \quad (5)$$

The heat generation term is written according to the Ohm-Fourier law, assuming a voltage gradient in only the axial direction as

$$\mathbf{i} \cdot \nabla E = -k_m \left(\frac{\partial E}{\partial z} \right)^2 \quad (6)$$

and if a linear voltage gradient is assumed

$$\mathbf{i} \cdot \nabla E = k_m \left(\frac{E}{L} \right)^2 \quad (7)$$

Substituting Eq. (7) into Eq. (2) gives, in dimensionless form,

$$\frac{1}{r^*} \frac{\partial}{\partial r^*} \left(r^* \frac{\partial T^*}{\partial r^*} \right) - \left(\frac{r_b^2}{\alpha t} \right) \frac{\partial T^*}{\partial z^*} + 4 = 0 \quad (8)$$

$$T^* = 0 \text{ at } z^* = 0 \quad (9)$$

$$T^* = 0 \text{ at } r^* = 1 \quad (10)$$

$$T^* = 0 \text{ at } r^* = r_a/r_b = r_0^* \quad (11)$$

It is assumed that the solution to Eq. (8) can be written as

$$T^*(r^*, z^*) = T_\infty^*(r^*) - T_i^*(r^*, z^*) \quad (12)$$

where the first term on the right represents the fully developed temperature profile and the second term on the right represents the deviation from a fully developed profile.

The fully developed solution can be obtained by setting the second term on the left-hand side of Eq. (8), representing axial convection, equal to zero and then integrating directly to give

$$T_\infty^* = \left[(1 - r^{*2}) + (r_0^{*2} - 1) \frac{\ln r^*}{\ln r_0^*} \right] \quad (13)$$

The solution representing the developing profile is obtained using the method of separation of variables and is given in terms of Bessel functions as

$$T_i^* = \sum_{n=1}^{\infty} A_n \exp \left(-\frac{\alpha \tau}{r_b^2} \lambda_n^2 \right) \Phi_n(r^*) \quad (14)$$

where

$$A_n = \frac{\int_1^{r_0^*} \left((1 - r^{*2}) + (r_0^{*2} - 1) \frac{\ln r^*}{\ln r_0^*} \right) \Phi_n(r^*) r^* dr^*}{2 [J_0^2(\lambda_n) - J_0^2(\lambda_n r_0^*)]} \frac{1}{\pi^2 \lambda_n^2 J_0^2(\lambda_n r_0^*)} \quad (15)$$

and

$$\Phi_n(r^*) = Y_0(\lambda_n)J_0(\lambda_n r^*) - Y_0(\lambda_n r^*)J_0(\lambda_n) \quad (16)$$

The eigenvalues λ_n are evaluated from the characteristic equation

$$\Phi_n(r_0^*) = Y_0(\lambda_n)J_0(\lambda_n r_0^*) - Y_0(\lambda_n r_0^*)J_0(\lambda_n) = 0 \quad (17)$$

The constants A_n are evaluated by numerical integration. Generally, only 2 to 3 terms in the summation of Eq. (14) are required since the exponential term diminishes rapidly with increasing size of the eigenvalues.

Substitution of Eqs. (13) and (14) into Eq. (12) gives the temperature profile in the CRAE column as

$$T^* = \left[(1 - r^{*2}) + (r_0^{*2} - 1) \frac{\ln r^*}{\ln r_0^*} \right] - \sum_{n=1}^{\infty} A_n \Phi_n(r^*) \exp\left(\frac{-\alpha\tau}{r_b^2} \lambda_n^2\right) \quad (18)$$

The dimensionless temperature is thus a function of the dimensionless radial position (r^*), the ratio of outer to inner radius (r_0^*), and the Fourier number, ($Fo = \alpha\tau/r_b^2$, where τ is a function of z^*). Temperature profiles as a function of the Fourier number are shown in Fig. 3.

Power Requirements

The power required for a given separation using annular electrophoresis is given by the expression

$$P = 2\pi \int_{r_b}^{r_a} (\mathbf{i} \cdot \nabla E) r dr \quad (19)$$

Substituting Eq. (7) for the power density and integrating, the power consumed is

$$P = \pi(r_a^2 - r_b^2)k_m \left(\frac{E^2}{L} \right) \quad (20)$$

Separation Distance

Electrophoretic separations occur because of the uniqueness of a charged substance's electrophoretic mobility. Depending upon the

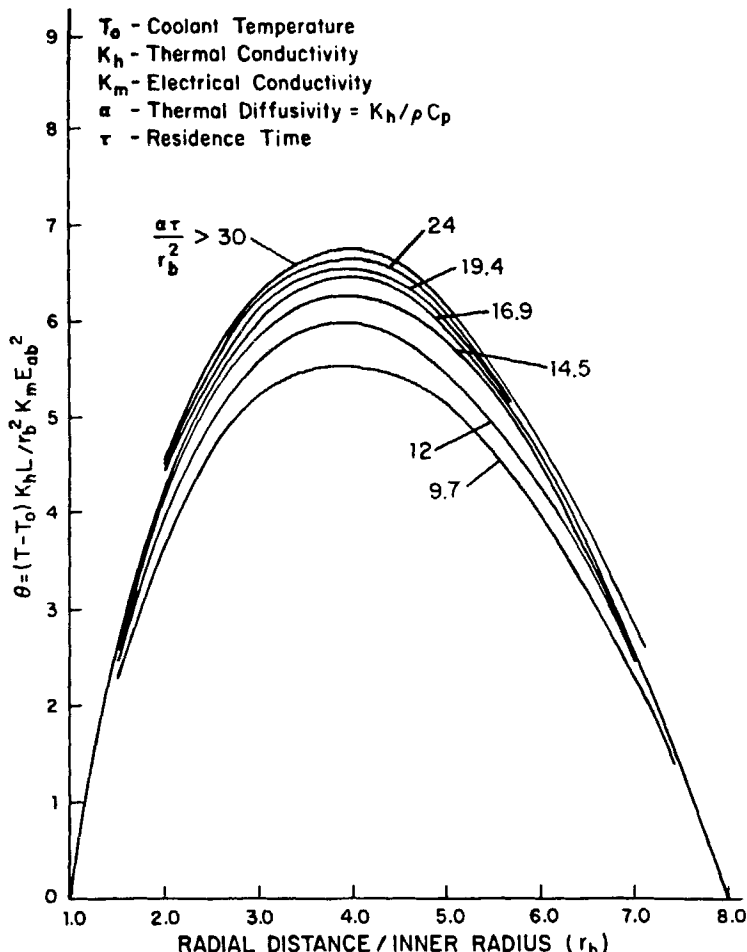


FIG. 3. Calculated dimensionless temperature profiles in a CRAE column with an outer to inner radius ratio of 8.

charged state of the substance, the charged particle migrates with a velocity proportional to the voltage applied in the electric field toward the electrode of opposite charge. The retention time for species i is given by

$$t_i = L/v_i \quad (21)$$

Assuming unidirectional flow, the total velocity is a sum of the convective and electromigration velocity:

$$v_i = v_{mig,i} + \langle v \rangle \quad (22)$$

The velocity due to convection is the average velocity of the eluent and is given by

$$\langle v \rangle = L/\tau \quad (23)$$

where τ is the mean residence time of the eluent. The velocity due to electromigration is proportional to the voltage gradient applied over the bed and is given by

$$v_{mig,i} = u_i \left(\frac{\partial E}{\partial z} \right) = u_i \left(\frac{E}{L} \right) \quad (24)$$

The distance traveled in the angular direction by species i is given by

$$S_i = r_f \omega t_i \quad (25)$$

The separation distance between two components is then

$$\Delta S_{ij} = r_f \omega (t_i - t_j) \quad (26)$$

Using Eq. (23), Eq. (25) becomes

$$\Delta S_{ij} = r_f \omega L^2 \tau \left(\frac{1}{u_i E \tau + L^2} - \frac{1}{u_j E \tau + L^2} \right) \quad (27)$$

Bandspeading

In electrophoretic devices, it is often assumed that a species disperses such that the concentration follows a Gaussian distribution (18). Under these conditions, the concentration is given by

$$c^* = \frac{c}{c^\circ} = \frac{1}{(4\pi D t)^{1/2}} \exp \left(\frac{-x^2}{4Dt} \right) \quad (28)$$

where c° is the total material diffusing and the variance $\sigma^2 = 2Dt$.

Of a given species, 99% can be expected to elute within 2.5σ of the mean angular distance. Thus, if we insist that each species' mean angular distance be at least 5σ apart, we can be assured of reasonably pure

products. For example, if the diffusivity is assumed to be that of a typical small protein (10^{-5} cm 2 /s) and the residence time is 2 h, the diffusion distance is about 0.9 cm. We should then require a separation distance of at least 1.8 cm to achieve pure separation.

This result is encouraging as it indicates that the CRAE design has sufficient resolving power to achieve practical separations. It should be noted, however, that additional bandspeading is expected to occur in the actual device due to electroosmosis and hydrodynamic effects, especially those resulting from thermal gradients. The effect of the temperature gradient on the bulk velocity profile has been investigated (45). It was found that the temperature dependence of the physical properties could significantly influence bulk flow patterns in an annulus. Thus, the change in the density and, more importantly, the viscosity as a function of the temperature gradient will lead to additional bandspeading. Further, the effect of temperature on electrokinetic parameters and migrational velocity will also lead to band asymmetry and spreading. These electromigrational dispersion effects have been shown to be as significant as simple diffusional effects (46).

DISCUSSION

The design and performance of the CRAE column depends upon several factors: the components, the pH of the eluent, the minimum separation distance desired, and the maximum temperature allowable within the column. Other effects including electroosmosis, hydrodynamic effects, migrational effects, thermal gradients, and system geometry all play a role in bandspeading and were not included in this analysis. These complex physical processes, although significant, are ignored for the time being in order to focus attention on the essential aspects of the CRAE column and to demonstrate its basic feasibility for electrophoretic separations.

The separation of glycine from glutamic acid is used to demonstrate the column design and is chosen so that the results might be directly compared with the annular column developed by Vermeulen and coworkers. Vermeulen's column was also of a thick bed, annular geometry designed for large-scale processing and, therefore, more similar to the CRAE column than existing low throughput, thin channel, rectangular Hannig-type units. A pH of 6.9 and a residence time of 2 h are assumed for example purposes.

Peak Temperature Rise

An important design constraint in an electrophoresis column is the peak bed temperature since many proteins will denature at 50–60°C. The peak temperature rise can be estimated from information about the required power consumption, residence time, necessary separation distance, bed thickness, and column volume. The relationship between these parameters and the peak temperature rise for the CRAE column is shown in Figs. 4a-d for different power consumption but for the same volume and residence time. For a given power, the peak temperature rise increases steeply as the required separation distance increases. The rate of increase is largest for smaller inner radius and diminishes as inner radius increases. The effect of bed thickness on the peak temperature rise is indicated by the horizontal lines in Fig. 4. Bed thickness appears to have little effect on the peak temperature rise when the ratio of the outer radius to the inner radius is less than 2. However, when the ratio is greater than 3, substantial temperature rise is seen, especially at long residence times, as seen in Fig. 5. As the ratio of outer to inner radius increases, the surface area to volume ratio decreases, resulting in diminished heat transfer and a concurrent rise in bed temperature. The relationship between unit power and separation distance as a function of residence time is shown in Fig. 6. As an example, consider a CRAE column with a residence time of 2 h, outer diameter of 70 cm, column length of 50 cm with a volume of 50 L and a required separation distance of 4.5 cm. From Fig. 6, the power consumed will be 0.014 W/cm³. For a volume of 50 L, the total power consumed is 700 W. From Fig. 4d, using an inner radius of 30 cm, the peak temperature rise will be approximately 5°C. The radial position where the maximum temperature occurs can be determined from Fig. 7. For a temperature rise of 5°C, the dimensionless temperature is 0.014. Figure 7 gives the radial position of the peak temperature as about 32.4 cm.

Separation Distance

The separation distance as a function of peak temperature is presented in Figs. 4a-d for various column dimensions, and as a function of applied voltage in Fig. 8 for a glycine–glutamic acid separation. For fixed radii and volume, as the residence time increases, the bed length increases and the required separation distance increases. Clearly, long

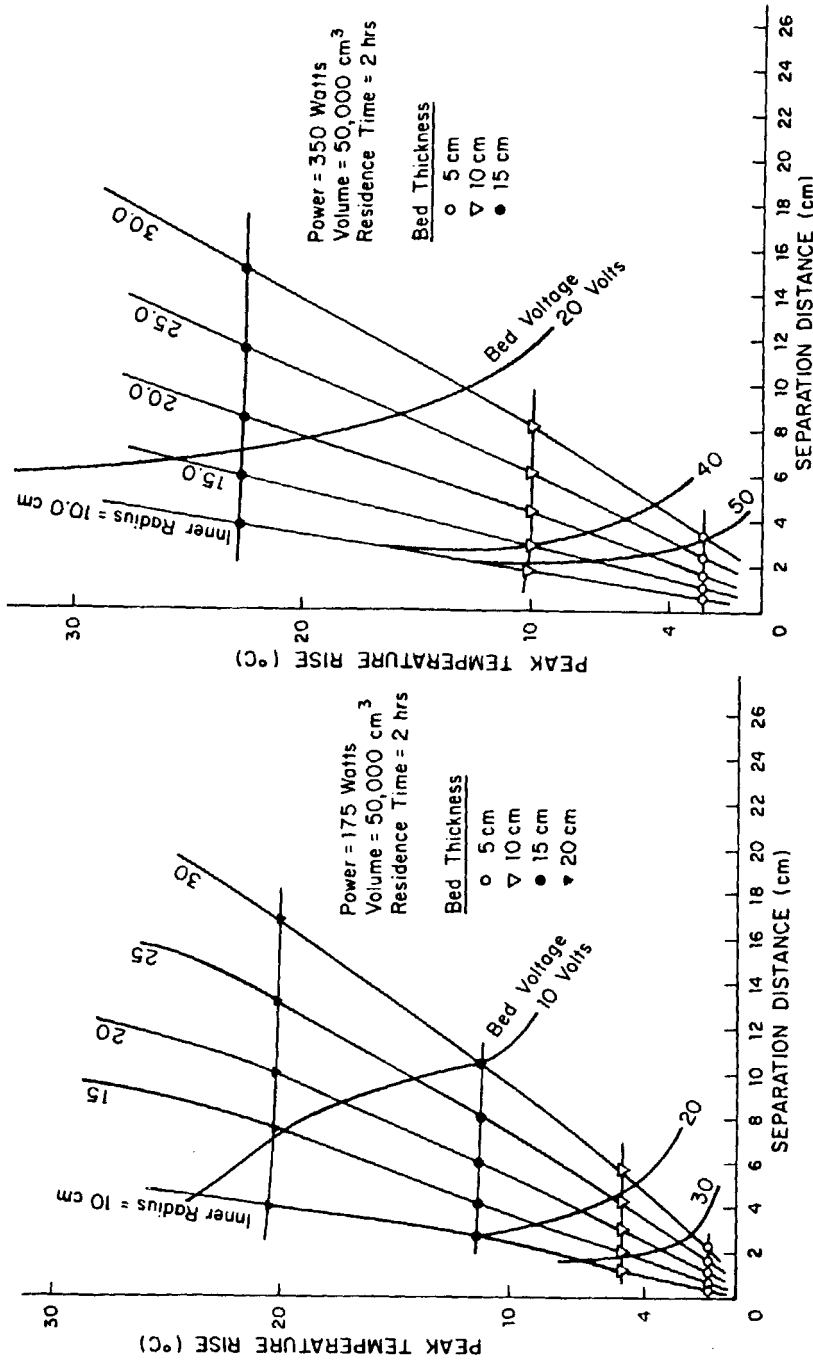


FIG. 4a. Calculated peak temperature rise as a function of separation distance and bed voltage for various CRAE column designs of the same volume and residence time. 175 W.

FIG. 4b. As for Fig. 4a but with 350 W.

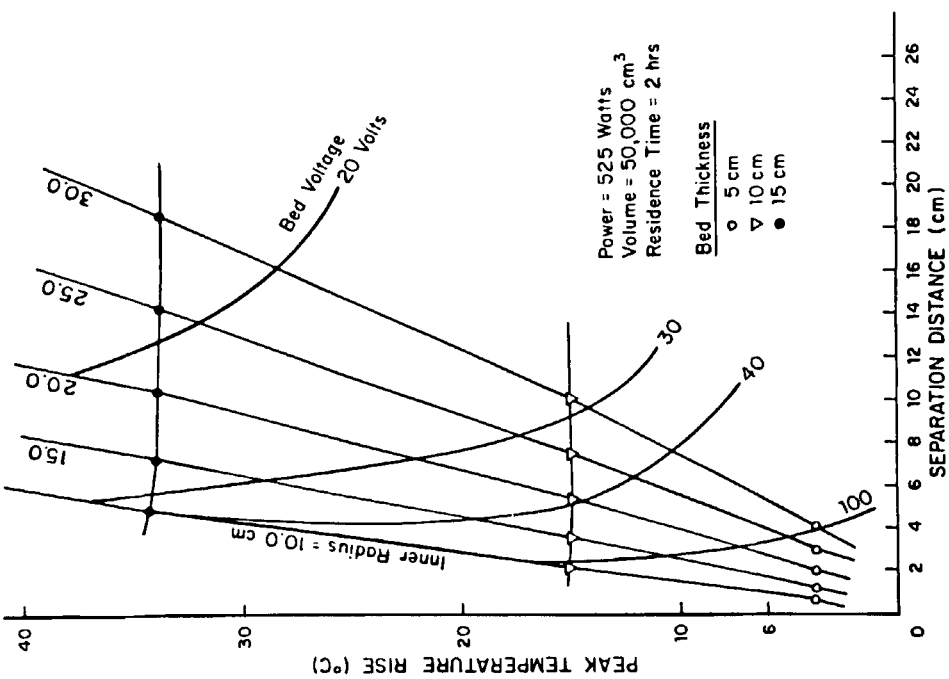


FIG. 4c. As for Fig. 4a but with 525 W.

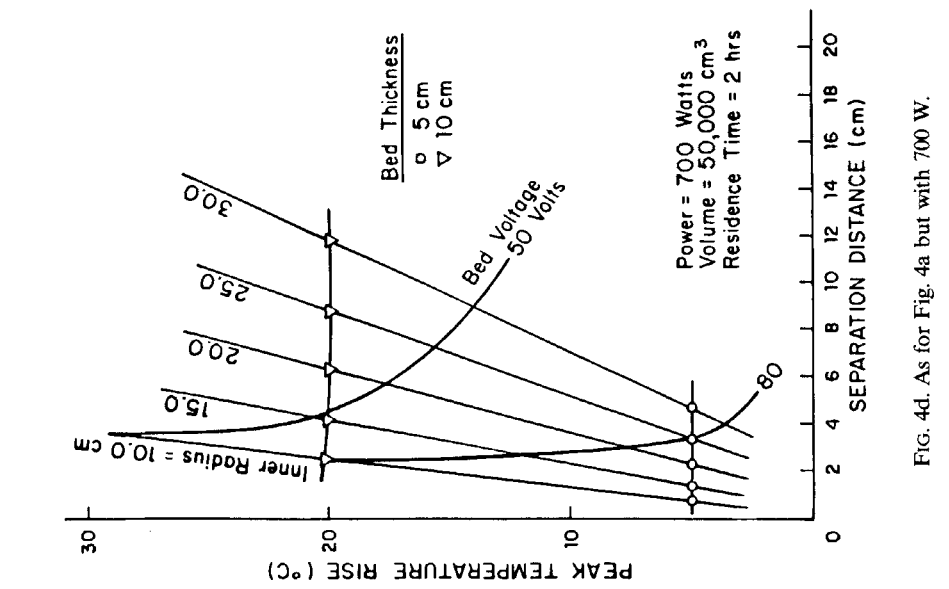


FIG. 4d. As for Fig. 4a but with 700 W.

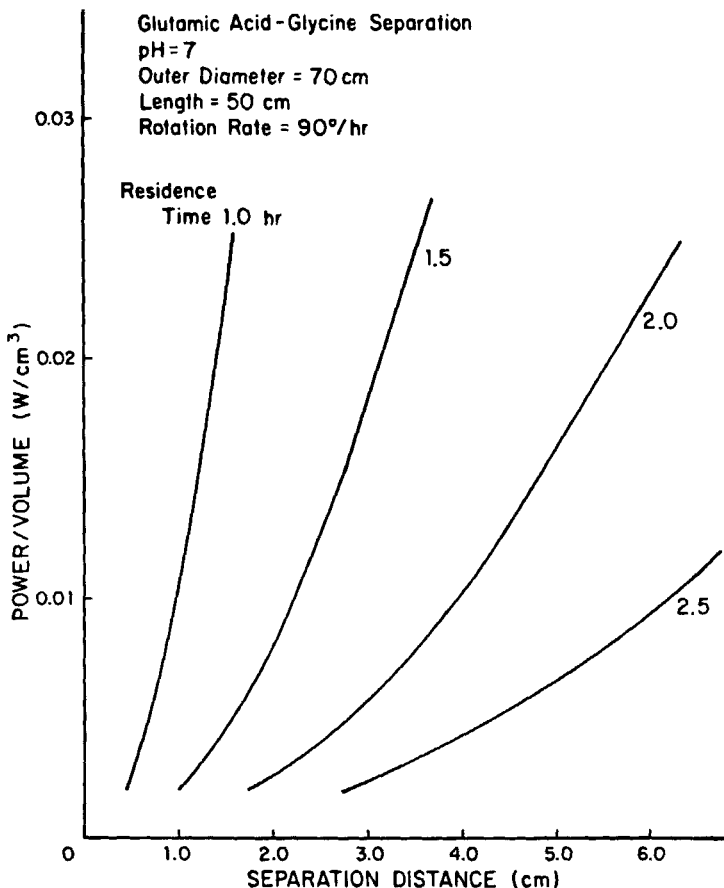


FIG. 5. Relationship between power and separation distance as a function of residence time for a glycine-glutamic acid separation in a CRAE column.

residence times will cause increased bandspreading by diffusion. The relationship between the separation factor, defined as the ratio of electrophoretic mobilities between two species, and the residence time and the separation distance is shown in Fig. 9. For example, for a residence time of 2 h and a required separation distance of 4 cm, the species must have a separation factor of at least 2.8. Furthermore, due to other effects mentioned previously, the separation distances obtained from these figures must be considered minimum.

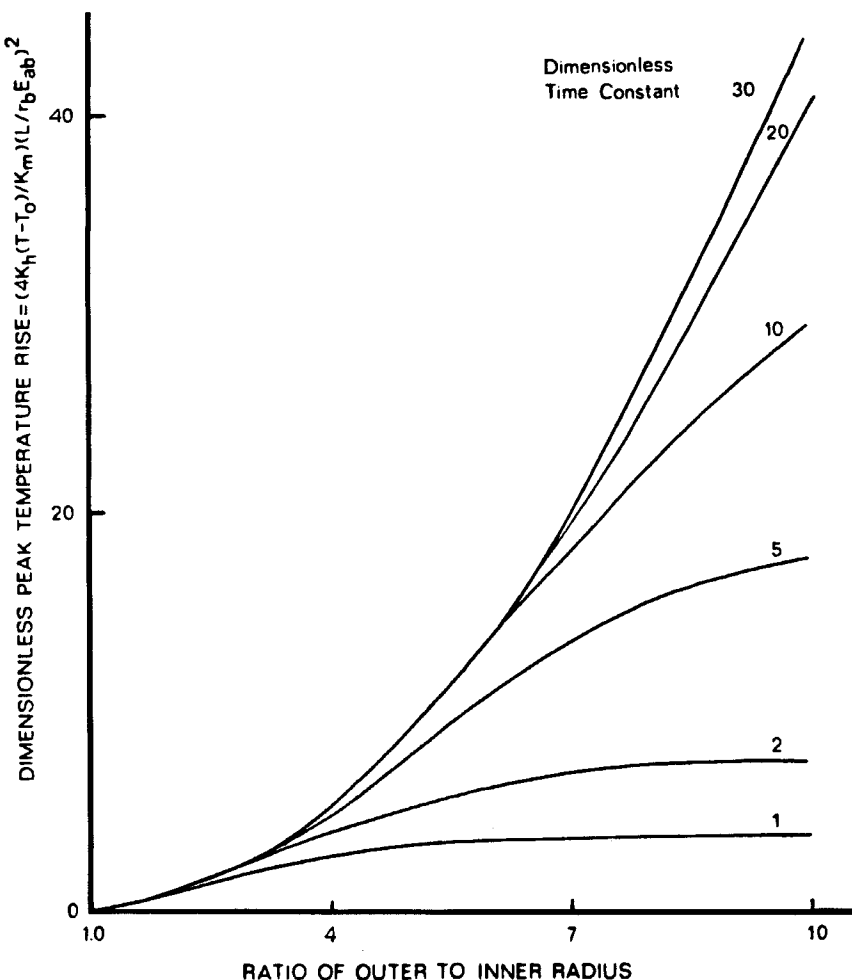


FIG. 6. Dimensionless peak temperature rise as a function of outer to inner radius ratio and dimensionless time constant for the CRAE column.

Comparison of CRAE Column Performance

A comparison of the performance of various CRAE column designs with that of the stationary column developed by Vermeulen and coworkers for a glycine-glutamic acid system is presented in Table 1.

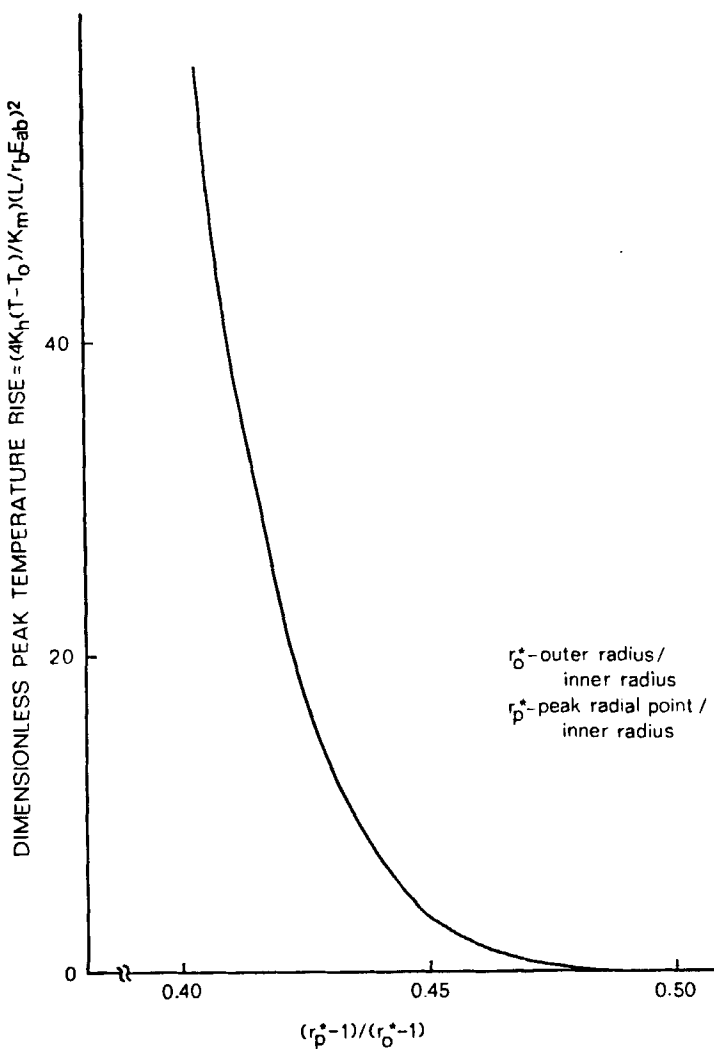


FIG. 7. Location of peak temperature in the CRAE column.

Assuming that the capital cost of simple annular columns is roughly a function of volume, all units simulated would not differ significantly from one another in capital cost. On the other hand, operating cost would be proportional to power consumed. On this basis, the CRAE columns will be significantly less expensive than the Vermeulen column. In addition, the CRAE columns are capable of maintaining a maximum temperature rise of 5°C compared to 27.5°C for the Vermeulen column. The CRAE column is also able to achieve higher separation distances.

In Cases B, C, and D, the physical size is held constant while increasing the applied voltage. As expected, power consumption and temperature rise increases as well as the separating ability, as indicated by the increase in separation distance. Case A uses a thicker annulus than the other cases and has a comparable separation distance and peak temperature rise. The annular bed design of the CRAE column allows the annulus thickness to be specified separately from the inner column radius. Note that the heat transfer area is related to the column radius, whereas the heat transfer resistance of the bed is a function of the annulus thickness. In cases where the thermal resistance of the bed dominates the heat transfer mechanism, the CRAE column offers greater flexibility in design and scale-up.

TABLE 1
Representative Results of the Continuous Rotating Electrophoresis Column for
Glycine-Glutamic Acid Separation

	A ^a	B	C	D	Vermeulen's design
Volume (L)	50	50	50	50	37.7
Power (W)	175	350	525	700	712
Residence time (s)	7200	7200	7200	7200	7200
Bed voltage (V)	18.1	47.2	57.8	66.0	16
Separation distance (cm)	4.3	3.3	4.0	4.7	2.3
Peak temperature rise (°C)	5.0	2.5	3.7	5.0	27.5

	Dimensions (cm)		
	Inner radius	Outer radius	Length
A	25.0	35.0	26.5
B	30.0	35.0	49.0
C	30.0	35.0	49.0
D	30.0	35.0	49.0
Vermeulen's	1.25	10.0	122

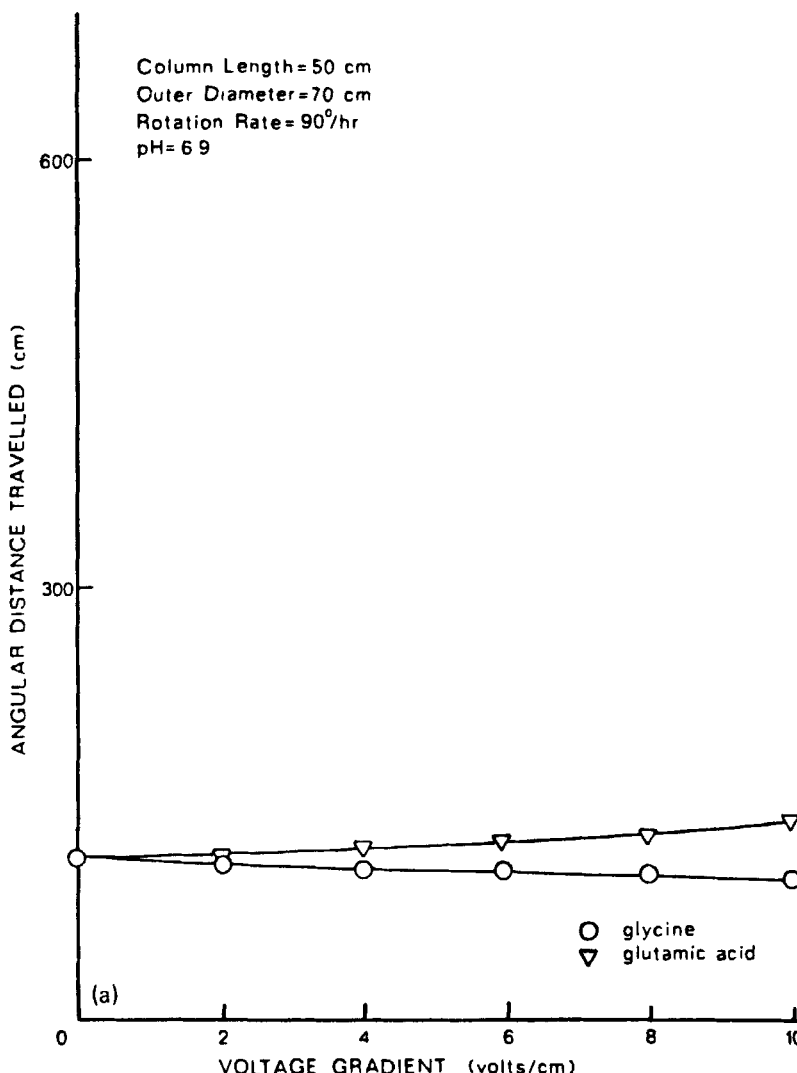
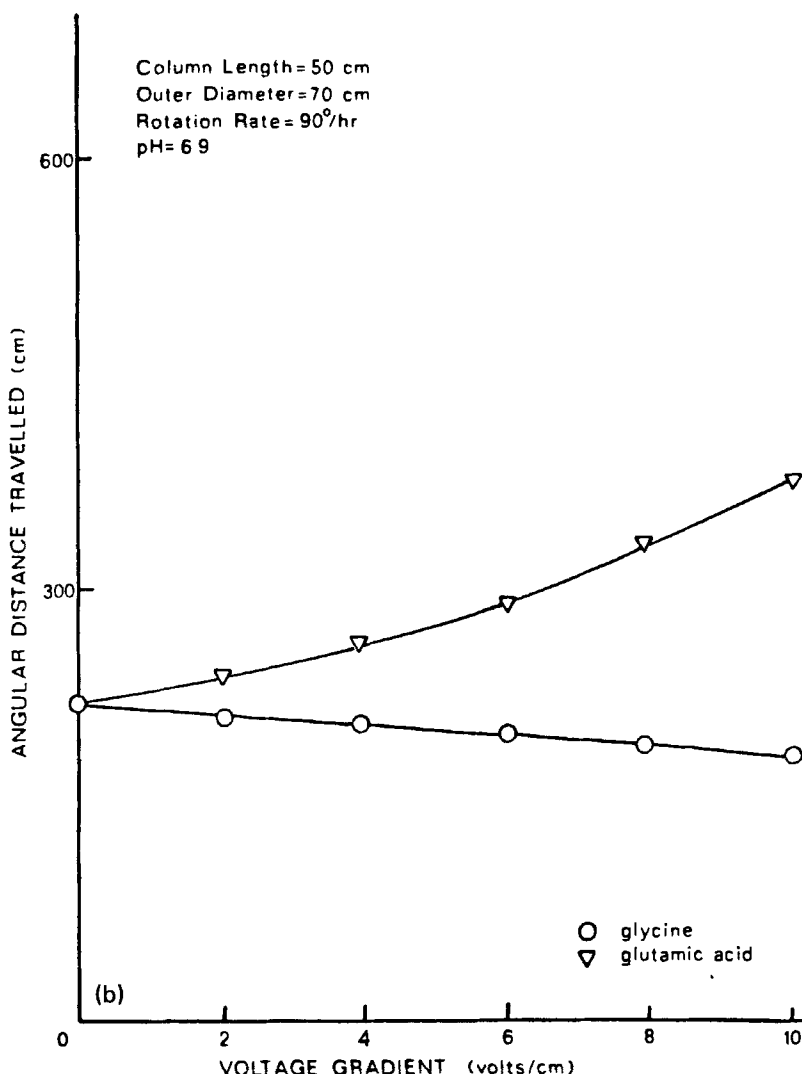


FIG. 8. Separation distance for glycine-glutamic acid system as a function of voltage gradient in the CRAE column. (a) Residence time = 2 h. (b) Residence time = 4 h.



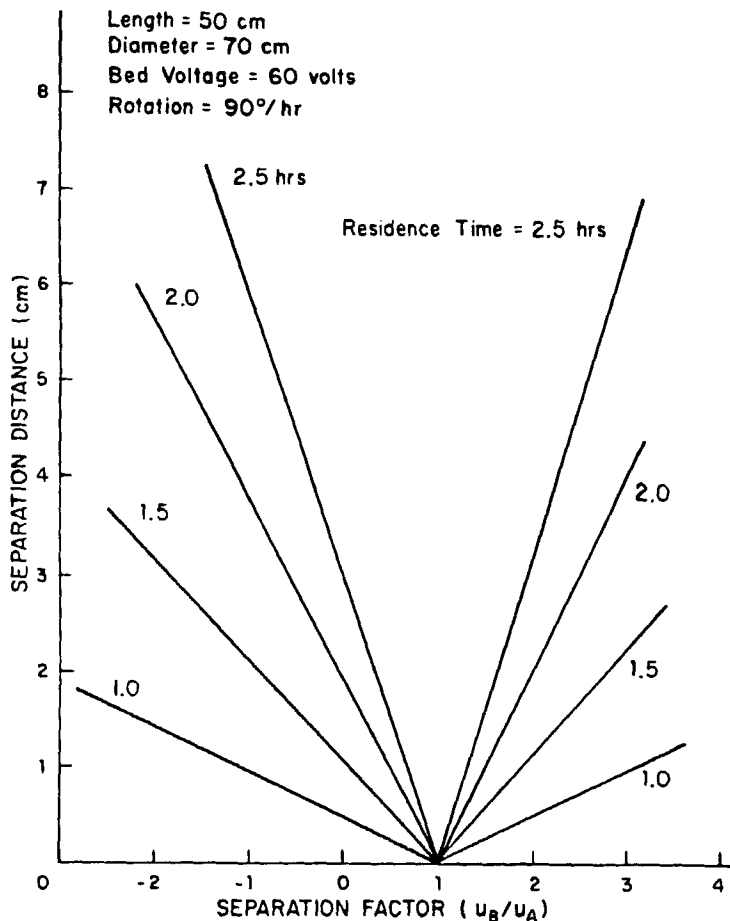


FIG. 9. Separation distance as a function of separation factor (basis: $u_a = -1.0 \times 10^{-4} \text{ cm}^2/\text{V} \cdot \text{s}$) and residence time for the CRAE column.

CONCLUSIONS

The preliminary analysis for the development of the continuous rotating annular electrophoresis (CRAE) column indicates that advantages in separating ability, temperature rise, and power requirements are gained by rotating the column and applying the electric field in the axial direction. In addition, the continuous rotating annular electrophoresis column offers potential benefits in that;

- The process is continuous.
- It can be scaled-up for industrial application.
- There is high resolution of products.
- Rotation allows the migration path to be lengthened without increasing the annular bed width.
- The annular bed width can be made thin so as to improve heat transfer and temperature control.
- There can be a large number of product collection points, depending upon the column diameter.
- The feed and product points are all stationary.
- The column can incorporate chromatography packing, thereby combining the separation advantages of chromatography with electrophoresis (electrochromatography).

A more rigorous model of the CRAE column is under development to include the effects of electroosmosis, natural convection, and nonuniform flow profiles on bandspreading. The second generation model will be validated with experimental data from a small-scale CRAE column. The results will then be compared with other electrophoresis designs including Hannig-type devices and the new Philpot/Harwell unit to determine the advantages and disadvantages of each design. The purpose of this paper is to introduce the concept of the CRAE column as being different from previous electrophoresis devices and to illustrate the potential merits of this new design.

SYMBOLS

A_n	temperature profile coefficient
C_p	heat capacity of eluent
c	concentration
D	molecular diffusivity

E	electrical potential
i	current density
J_0	Bessel function of zero order, first kind
k_h	effective thermal conductivity of bed
k_m	effective electrical conductivity of bed
L	length of column
P	power consumption
r	radial coordinate
r_a	radial position of outer cylinder
r_b	radial position of inner cylinder
r_f	radial position of feed inlet
r^*	dimensionless radial coordinate ($= r/r_b$)
r_0^*	dimensionless radial coordinate ($= r_a/r_b$)
S_i	distance traveled in the angular direction by i
ΔS_{ij}	separation distance in the angular direction between species i and j
T	temperature
T_c	characteristic temperature ($= k_m(r_b E/L)^2/4k_h$)
T_0	temperature of cooling water
T^*	dimensionless temperature ($= (T - T_0)/T_c$)
T_t^*	dimensionless developing temperature solution
T_∞^*	dimensionless fully developed temperature solution
t	time
t_i	retention time of species i
u_i	electrophoretic mobility of species i
v_i	total velocity of species i
$\langle v \rangle$	average velocity of eluent
$v_{mig,i}$	migration velocity
x	lateral coordinate
Y_0	Bessel function of zero order, second kind
z	axial coordinate
z^*	dimensionless axial transient solution
α	thermal diffusivity ($= k_h/\rho C_p$)
λ_n	eigenvalue
Φ	eigenvalue function
σ	standard deviation
σ^2	variance
ρ	density of eluent
τ	residence time
ω	angular velocity

REFERENCES

1. J. St. L. Philpot, "The Use of Thin Layers in Electrophoretic Separation," *Trans. Faraday Soc.*, **36**, 38-46 (1940).
2. V. R. Huebner and R. H. Lawson, "Performance Characteristics of a New Continuous-Flow Electrophoresis Instrument," *Sep. Sci. Technol.*, **3**, 265-277 (1968).
3. K. Hannig, "Continuous Free-Flow Electrophoresis as an Analytical and Preparative Method in Biology," *J. Chromatogr.*, **159**, 183-191 (1978).
4. K. Hannig, "New Aspects in Preparative and Analytical Continuous Free-Flow Cell Electrophoresis," *Electrophoresis*, **3**, 235-243 (1982).
5. M. Bier, O. A. Palusinski, R. A. Mosher, and D. A. Saville, "Electrophoresis: Mathematical Modeling and Computer Simulation," *Science*, **219**, 1281-1287 (1983).
6. M. Bier (ed.), *Electrophoresis: Theory, Methods, and Applications*, Vol. 1, Academic, New York, 1959.
7. M. Bier (ed.), *Electrophoresis: Theory, Methods, and Applications*, Vol. 2, Academic, New York, 1967.
8. Z. Deyl, F. M. Everaerts, Z. Prusik, and P. J. Svendsen (eds.), *Electrophoresis: A Survey of Techniques and Applications*, Pt. A, Techniques; Pt. B, Applications, Elsevier, Amsterdam, 1979.
9. P. G. Righetti, C. J. van Oss, and J. W. Vanderhoff (eds.), *Electrokinetic Separation Methods*, Elsevier/North Holland Biomedical Press, Amsterdam, 1979.
10. A. T. Andrews, *Electrophoresis: Theory, Techniques, and Biochemical and Clinical Applications*, Clarendon Press, Oxford, 1983.
11. C. F. Simpson and M. Whittaker (eds.), *Electrophoretic Techniques*, Academic, New York, 1983.
12. R. Dobry and R. K. Finn, "Engineering Problems in Large-Scale Electrophoresis," *Chem. Eng. Prog.*, **54**(4), 59-63 (1958).
13. A. Strickler and T. Sacks, "Continuous Free-Flow Electrophoresis: The Crescent Phenomena," *Prep. Biochem.*, **3**, 269-277 (1973).
14. A. Strickler and T. Sacks, "Focusing in Continuous-Flow Electrophoresis Systems by Electrical Control of Effective Cell Wall Zeta Potentials," *Ann. N. Y. Acad. Sci.*, **209**, 497-514 (1973).
15. J. F. G. Reis, E. N. Lightfoot, and H.-L. Lee, "Concentration Profiles in Free-Flow Electrophoresis," *AICHE J.*, **20**, 362-368 (1974).
16. K. Hannig, H. Wirth, B.-H. Meyer, and K. Zeiller, "Theoretical and Experimental Investigations of the Influence of Mechanical and Electrokinetic Variables on the Efficiency of the Method," *Hoppe-Seyler's Z. Physiol. Chem.*, **356**, 1209-1223 (1975).
17. F. E. P. Mikkers, F. M. Everaerts, and Th. P. E. M. Verheggen, "Concentration Distributions in Free Zone Electrophoresis," *J. Chromatogr.*, **169**, 1-10 (1979).
18. A. C. Arcus, A. E. McKinnon, J. H. Livesey, W. S. Metcalf, S. Vaughn, and R. B. Keey, "Continuous-Flow, Support-Free, Electrophoretic Separation in Thin Layers: Towards Large-Scale Operation," *Ibid.*, **202**, 157-177 (1980).
19. K. Hannig, "Die tragerfreie kontinuierliche Electrophoreses und ihre Anwendung," *Z. Anal. Chem.*, **181**, 244-254 (1961).
20. K. Hannig, "Preparative Electrophoresis," in *Electrophoresis: Theory, Methods, and Applications*, Vol. 2 (M. Bier, ed.), Academic, New York, 1967, pp. 423-471.
21. A. Strickler, "Continuous Particle Electrophoresis: A New Analytical and Preparative Capability," *Sep. Sci. Technol.*, **2**, 335-355 (1967).

22. A. R. Thompson, "Free-flow Electrophoresis," in *Electrophoretic Techniques* (C. F. Simpson and M. Whittaker, eds.), Academic, New York, 1983, pp. 253-274.
23. R. M. Hybarger, C. W. Tobias, and T. Vermeulen, "Design Principles for Annular-Bed Electrochromatography," *Ind. Eng. Chem., Process Des. Dev.*, 2, 65-71 (1963).
24. T. Vermeulen, L. Nady, J. M. Krochta, E. Ravoo, and D. Howery, "Design Theory and Separations in Preparative Scale Continuous Flow Annular Bed Electrophoresis," *Ibid.*, 10, 91-102 (1971).
25. R. Dobry and R. Finn, "New Approach to Continuous Electrophoresis," *Science*, 127, 697-698 (1958).
26. S. Ostrach, "Convection in Continuous-Flow Electrophoresis," *J. Chromatogr.*, 140, 187-195 (1977).
27. D. A. Saville, "Fluid Mechanics of Continuous Flow Electrophoresis," *Space Res.*, 19, 583-597 (1979).
28. D. A. Saville, "The Fluid Mechanics of Continuous Flow Electrophoresis in Perspective," *Phys. Chem. Hydrodynam.*, 1, 297-307 (1980).
29. P. Mattock, G. F. Aitchison, and A. R. Thompson, "Velocity Gradient Stabilized, Continuous, Free Flow Electrophoresis," *Sep. Pur. Methods*, 9, 1-68 (1980).
30. J. B. Fox, R. C. Calhoun, and W. J. Eglinton, "Continuous Chromatography Apparatus, Part I, Construction," *J. Chromatogr.*, 43, 48-54 (1969).
31. J. B. Fox, "Continuous Chromatography Apparatus, Part II, Operation," *Ibid.*, 43, 55-60 (1969).
32. R. A. Nicholas and J. B. Fox, "Continuous Chromatography Apparatus, Part III, Application," *Ibid.*, 43, 61-65 (1969).
33. C. D. Scott, R. D. Spence, and W. G. Sisson, "Pressurized Annular Chromatograph for Continuous Separations," *Ibid.*, 126, 381-400 (1976).
34. J. M. Begovich, "Multicomponent Separations using a Continuous Annular Chromatograph," PhD Dissertation, University of Tennessee, Knoxville, Tennessee, 1982.
35. J. M. Begovich and W. G. Sisson, "A Rotating Annular Chromatograph for Continuous Metal Separations and Recovery," *Res. Cons.*, 9, 219-229 (1982).
36. J. M. Begovich and W. G. Sisson, "A Rotating Annular Chromatograph for Continuous Separations," *AIChE J.*, 30, 705-709 (1984).
37. P. C. Wankat, "The Relationship between One-Dimensional and Two-Dimensional Separation Processes," *Ibid.*, 23, 859-867 (1977).
38. P. C. Wankat, "Two-Dimensional Separation Processes," *Sep. Sci. Technol.*, 19, 801-829 (1985).
39. J. O. N. Hinkley, "Electrophoretic Thermal Theory, Pt. I, Temperature Gradients and Their Effects," *J. Chromatogr.*, 109, 209-217 (1975).
40. J. F. Brown and J. O. N. Hinkley, "Electrophoretic Thermal Theory, Pt. II, Steady-State Radial Temperature Gradients in Circular Section Columns," *Ibid.*, 109, 218-224 (1975).
41. E. D. Lynch and D. A. Saville, "Heat Transfer in the Thermal Entrance Region of an Internally Heated Flow," *Chem. Eng. Commun.*, 9, 201-211 (1981).
42. R. S. Turk and C. F. Ivory, "Temperature Profiles in Plane Poiseuille Flow with Electrical Heat Generation," *Chem. Eng. Sci.*, 39, 851-857 (1984).
43. R. J. Naumann and P. H. Rhodes, "Thermal Considerations in Continuous Flow Electrophoresis," *Sep. Sci. Technol.*, 19, 51-75 (1984).
44. L. M. Korndorf, "Mathematical Analysis of Continuous Rotating Annular Electrophoresis," MS Thesis, University of Iowa, Iowa City, Iowa, 1984.
45. H. L. Zingher, "Numerical Analysis of Velocity Profiles in a Continuous Rotating

Annular Electrophoresis Column," MS Thesis, University of Iowa, Iowa City, Iowa, 1985.

46. W. Thormann, "Description and Detection of Moving Sample Zones in Zone Electrophoresis: Zone Spreading Due to the Sample as a Necessary Discontinuous Element," *Electrophoresis*, 4, 383-390 (1983).

Received by editor December 5, 1985

Revised March 3, 1986